NUMERICAL APPROACH TO THE OVERLAND FLOW PROCESS IN VEGETATIVE FILTER STRIPS

R. Muñoz-Carpena, J. E. Parsons, J. W. Gilliam
STUDENT MEMBER ASAE, MEMBER ASAE

ABSTRACT. *Agricultural and other disturbed lands contribute to non-point source pollution of water bodies (streams and lakes). Vegetative filter strips (VFS) are often recommended to reduce off-site impacts. Design guidelines to optimize the performance of VFS are not readily available. A process-based model is presented to simulate the hydrology of a Vegetative Filter Strip for a given event. The model consists of a quadratic finite element overland flow submodel, based on the kinematic wave approximation, coupled with an infiltration submodel based on a modification of the Green-Ampt equation for unsteady rainfall. The model is used to study the effect of soil type, slope, surface roughness, buffer length, storm pattern and field inflow on the VFS performance. Filter performance, i.e., reduction of the runoff volume, velocity and peak, is higher for denser grass cover, smaller slopes and soils with higher infiltration capacity. Time to peak(s) depended mainly on the roughness-slope combination.* ***Keywords.*** *Vegetative filter strips, Flow, Modeling.*

The sediment leaving disturbed areas, besides being a pollutant itself, can carry nitrogen and phosphorus into water ecosystems, thereby accelerating eutrophication of lakes (Flanagan et al., 1989). In many cases, conservation management practices and structures can reduce off-site impacts. One such accepted management practice is vegetative filter strips (VFS) which are bands of planted or indigenous vegetation that may control transport of sediment and reduce non-point source pollution off-site. Vegetation reduces surface runoff by increasing infiltration, augmenting roughness of the soil surface, boosting evapotranspiration, and contributing to rainwater interception. Both the retardation of flow and reduction in runoff discharge reduce the kinetic energy of runoff, and thus lower the sediment transport capacity (Foster, 1982). Sediment-bound nutrients are removed from runoff in these vegetative zones as sediment is deposited (Flanagan et al., 1989). For nutrients attached to sediment, the deposition process largely controls the effectiveness of the buffer area. For soluble nutrients, infiltration is the controlling factor.

Parsons et al. (1990) showed that large reductions of runoff from an adjacent field are experienced in buffers. The length of the filter is an important factor in its performance, as are other parameters such as slope, surface roughness, and soil type. An appropriate means of determining optimal placement, dimensions, and arrangements of buffer areas must be developed if they are to be effective and economical (Swift, 1986). In evaluating the effectiveness of VFS and riparian areas, it is desirable to identify those characteristics which affect the efficiency of nutrient and sediment reduction.

This study deals with modeling the surface flow component in VFS and evaluating the effect of a number of parameters on surface runoff hydrographs. The model developed is width-averaged, which translates into a one-dimensional (1-D) approach. The solutions obtained from the formulation are given in terms of unit width of surface (in the direction of the movement of the flood wave). This technique is especially useful in the VFS problem where the surface to model is a band of vegetation of a certain width and an extension of results would be desirable for other widths as well. Grass and other uniform soil covers fit the assumptions of this approach. The objective of this modeling approach is the design of strips, not the management of the areas, i.e., specify required strip lengths to give specific runoff reductions. The "state of the art" in specifying buffer strip requirements indicates that this process-based approach will provide a check for approximate methods and a better understanding of the processes involved.

BACKGROUND

Overland flow routing describes the water movement over the land surface and implies the calculation of flow rates at positions along the hillslope (Lane et al., 1987). The solution of the overland flow routing equation is needed for the sediment transport problem solution of interest in non-point source pollution studies. Proper representation of the land surface is the basic issue in modeling overland flow (Lane and Woolhiser, 1977). Foster and Meyer (1972) treated surfaces as areas of broad, uniform sheet flow dissected by areas of concentrated flow in rills. This approach is used in the WEPP hillslope model to predict runoff peak rate for unsteady, nonuniform flow (Lane et al., 1987). The kinematic approach of the WEPP model considers a total hydraulic resistance (f_r) as the

Article was submitted for publication in October 1992; reviewed and approved for publication by the Soil and Water Div. of ASAE in April 1993.

Paper No. BAE-92-12 of the Journal Series of the Department of Biological and Agricultural Engineering, North Carolina State University, Raleigh.

The authors are **Rafael Muñoz-Carpena**, Graduate Student, **John E. Parsons**, Assistant Professor, Biological and Agricultural Engineering Dept, and **J. Wendell Gilliam**, Professor, Soil Science Dept., North Carolina State University, Raleigh.

  0001-2351 / 93 / 3603-0761

summation of a soil friction factor, a microtopographic irregularities friction factor (random roughness), and friction factors due to residue and plant cover on the soil. This total f_r factor represents the total surface resistance to flow. WEPP can generate hydrographs, runoff rates with time, but the erosion component uses peak rates from a steady-state solution (Lane et al., 1987).

New efforts to account for variability of the land surface on the overland flow process can be found in the literature. Rawls and Brakensiek (1988) address the problem of surface variability in time and space in a model that accounts for the effect of management practices on infiltration. The model is a solution to the Green-Ampt equation for unsteady rainfall. One of the factors specifically included in the model is percentage of grass cover, its seasonal variation, and composition of this cover. Springer and Cundy (1988) consider the effects of excess rainfall generation on erosion. In particular they looked at the effects of spatial variation in saturated conductivity (K_s) on erosion resulting from overland flow. They used a mathematical routing model and concluded that overestimation errors of 9 to 45% are introduced by neglecting spatial variability of K_s. This error decreased as rainfall and antecedent moisture increased. However, this variability in K_s did not lead to differential deposition along the slope.

One important aspect of the field problem is finding the correct mass balance at the surface. To achieve this, infiltration must be considered. There are different alternatives among the existing models. The most exact approach is solving the governing partial differential equations for infiltration, i.e., some form of Richards' equation (1931), subject to the appropriate boundary and initial conditions. These solutions are computationally expensive and subject to numerical instabilities. Alternative models have been devised based on simplified concepts that lead to an algebraic formulation of the infiltration rate or cumulative infiltration in terms of time and soil parameters. Skaggs and Khaheel (1982) reviewed the empirical models of Kostiakov, Horton, Philip and Holtan, and the physically based models of Green-Ampt, Smith, and Smith-Parlange. Some comparative studies show that the fitness of the method employed varies greatly depending on the estimation of the parameters of each of the equations (Skaggs et al., 1969).

Panda et al. (1988) found that the cause of error in Green-Ampt infiltration models is often the estimates of antecedent water content. They proposed a model that overcomes this problem by providing a daily accounting of soil water content in the root zone, incorporating predictions of infiltration, evapotranspiration, and deep percolation for unsteady rainfall.

Cundy and Tento (1985), Stone et al. (1992) and Woolhiser et al. (1990) developed models that account for the interaction of overland flow and infiltration handled by the approximate methods of Philips, Green-Ampt, and Smith-Parlange, respectively. The first two models, however, consider the land area as a plane with only one inflow source, i.e., rainfall over the plane. This approach does not allow for the singularities of the VFS, namely, the inflow from some uphill field area is much larger than rainfall atop the buffer, and irregularities at the surface (changes in slope or roughness throughout the filter). The last model, KINEROS (Woolhiser et al., 1990), solves the problem as a series of cascade planes, and can be applied for the case of inflow from the field. This model is based on the finite difference, four-point implicit scheme solution to the kinematic wave equations.

The modeling effort developed herein is based on the numerical solution of the mathematical formulation of the surface water routing described by a set of partial differential equations (PDE) linked to the Green-Ampt infiltration model for unsteady rainfall.

Hydraulic Routing Submodel

Mathematical Formulation

The mathematical formulation of the one-dimensional (1-D) hydraulic routing process was first derived by Barre de Saint-Venant in 1881. It is based on a mass and momentum balance within a control volume (of unit width). For the 1-D case the general PDEs can be described as:

$$\frac{\partial h}{\partial t} + \frac{\partial q}{\partial x} = i_e = r - f \qquad (1)$$

$$\frac{\partial v}{\partial t} + v\frac{\partial v}{\partial x} + g\frac{\partial h}{\partial x} = g\left(S_o - S_f\right) - \frac{v i_e}{h} \qquad (2)$$

where

- x = flow direction axis (m)
- t = time scale (s)
- $h(x, t)$ = vertical flow depth (m)
- $q(x, t)$ = discharge per unit width (m^2/s)
- i_e = rainfall excess (m/s)
- r = rainfall intensity (m/s)
- f = infiltration rate (m/s)
- v = depth averaged velocity (m/s)
- g = gravitational constant (m/s^2)
- S_o = ted slope (m/m)
- S_f = friction slope
- q = vh

The kinematic wave equations result from simplification of the Saint-Venant equations. Lighthill and Whitham (1955) proposed that the hydrodynamic terms of the momentum equation were negligible for the case where no backwater effects occurred. In this case, the momentum equation results in $S_o = S_f$ and the relationship between q and h in equation 1 can be expressed by means of a uniform flow equation. One widely used relation for the overland flow case is Manning's equation (Bedient and Huber, 1988; Lane and Woolhiser, 1977; Woolhiser, 1975):

$$q = \alpha h^m = \frac{\sqrt{S_o}}{n} h^{5/3} \qquad (3)$$

where α and m are the parameters of the uniform flow equation and n = Manning's roughness coefficient dependent on soil surface condition and vegetative cover. Values for n for different surface types can be found in the literature (Engman, 1986; Woolhiser, 1975).

In a natural flood, two kinds of waves, kinematic and dynamic, originate. The dynamic waves propagate at a speed faster than the main flood wave. The celerity of the wave (c) is the speed associated with the dynamic wave (Bras, 1990):

$$c = \frac{\partial q}{\partial h} = \frac{5}{3}\frac{\sqrt{S_o}}{n} h^{2/3} \qquad (4)$$

The kinematic wave assumption (Henderson, 1966) is that the speed of the kinematic wave is equal to the velocity of the main flood wave, which is achieved when the Froude number (Fr) is less than 1.5, where:

$$Fr = \frac{v}{\sqrt{gh}} < 1.5 \qquad (5)$$

The kinematic postulation is violated for very flat (S_o < 0.002) or very steep slopes (S_o > 0.1). For overland flow processes, the dynamic wave fronts attenuate very rapidly (Fr < 1.5), and kinematic waves dominate the flood response (Henderson, 1966).

Woolhiser and Ligget (1967) analyzed characteristics of the rising overland flow hydrograph and found that the kinematic wave assumption is accurate to within 10% if:

$$k = \frac{LS_o}{F_r^2 h_o} > 10 \qquad (6)$$

where

k = kinematic number
L = length of the domain (m)
h_o = depth of the flow at the end of the domain at steady state condition (m)

The initial and boundary conditions (BC) of the PDE can be described as:

$$h(x,0) = 0; \qquad 0 \le x \le L$$

$$h(x,t) = h_{bc}; \qquad t > 0 \qquad (7)$$

Note that the boundary condition can be modified for different cases. One case is when no uphill inflow occurs, where $h_{bc} = 0$ at the beginning of the slope. A second case is constant inflow from an uphill region out of the domain ($x < 0$), then $h_{bc} > 0$. A more realistic case would be α varying BC where $h_{bc} = h_{bc}(t)$, depending on the hydrograph off the uphill adjacent field.

Parameters (friction coefficient, slope) are included in a that allow modifications of the flow by soil surface, irregular microtopography and vegetal cover (Lane et al., 1987).

The load in the PDE is rainfall excess, i_e. Schmid (1989) investigated the implicit assumption in the model that infiltration is independent of overland flow so that the weak coupling of both processes (i.e., infiltration influences runoff but not vice versa) is taken into account. He found that the errors introduced were in most cases smaller than 5% and always less than 11%. Compared to the uncertainty introduced by the soil data in his analysis, he concluded, this is an acceptable assumption.

Numerical Solution

Kinematic routing was first discussed by Horton (1945) and Izzard (1946), defined by Lighthill and Whitham (1955), and later used to model the overland flow process (Henderson and Wooding, 1964; Henderson, 1966; Brakensiek, 1967; Ligget and Woolhiser, 1967; Eagleson, 1970). Eggert (1987) generalized the analytical solution for overland flow with the kinematic wave method using the method of characteristics (MOC). Eggert's model describes the rate of flow off the end of a uniform slope subject to a sequence of different spatially-uniform, time-different, non-negative inflows. Others presented solutions for kinematic flow over an infiltrating plane (Cundy and Tento, 1985; Woods and Ibbitt, 1988; Stone et al., 1992; Woolhiser et al., 1990). They point out the necessity to account for variation in the parameters, spatially and temporally, of this model.

Several numerical procedures can be used to solve the mathematical formulation of the overland flow problem for the 1-D case. These methods include Lagrangian or variable grid methods, such as characteristics (MOC), and Eulerian or fixed grid methods, such as different forms of finite differences (FD), and finite elements (FE) methods. The ideal method for this type of hyperbolic partial differential equation would be MOC. However, the difficulties associated with the application of the method to a space varying domain, such as in a field situation, make the method difficult. On the other hand, some solutions from Eulerian methods are not stable and exhibit convergence problems for abrupt changes of the physical properties of the system, often referred to as kinematic shocks. Recent work, using Eulerian methods with refined spatial and temporal discretization and smoothed values of spatially variable parameters, avoids numerical errors associated with kinematic shocks (Ponce, 1991; Vieux et al., 1991). The use of non-standard FE method, i.e., quadratic Petrov-Galerkin FE, has also been presented as an effective means of reducing such errors (Muñoz-Carpena et al., 1993). The FE has been applied on several occasions to the 1-D problem (Judah, 1972; Ross, 1977; Ross et al. 1979a,b; Blandford and Meadows, 1990; Vieux, 1988; Vieux and Segerlind, 1989; Vieux et al., 1991).

A fundamental parameter for the numerical solution is the Courant number defined as:

$$Cr = \frac{c\,\Delta t}{\Delta x} \qquad (8)$$

where Δx and Δt are space and time increments. Implicit formulations, such as the one proposed, are unconditionally stable; however, as the value of Cr decreases, the accuracy of the solution increases, at the expense of computational time (Blandford and Meadows, 1990; Vieux et al., 1991).

Using the standard Galerkin finite element method, the weak energy formulation of equation 1 is expressed as:

$$\int_D W_i \left(\frac{\partial \hat{h}}{\partial t} + \frac{\partial \hat{q}}{\partial x} - i_e \right) dx = 0; \qquad \text{for } i = 1, n_n \qquad (9)$$

where W_i is a weight or test function at node i, $\hat{h}$ and $\hat{q}$ are approximations of h and q, based on a continuous distribution expressed in terms of the actual value at selected points (nodes), h_j:

$$\hat{h}(x) = \sum_{j=1}^{n_n} N_j(x)\, h_j$$

$$\hat{q}(x) = \sum_{j=1}^{n_n} N_j(x)\, q_j = \sum_{j=1}^{n_n} \alpha(x)\, N_j(x)\, h_j^{5/3} \qquad (10)$$

and

$$\frac{\partial \hat{q}(x)}{\partial x} = \frac{\partial}{\partial x}\left[\sum_{j=1}^{n_n} N_j(x)\, q_j\right] = \frac{dN_j}{dx}\, q_j \qquad (11)$$

n_n is the number of nodes in the domain and N_j are termed basis functions, standard Lagrange interpolation polynomials in natural coordinates ($-1 \le \xi \le 1$) for every element of the system:

$$N_j(\xi) = \prod_{\substack{n=1 \\ n \ne j}}^{3} \frac{(\xi - \xi_n)}{(\xi_j - \xi_n)} \qquad (12)$$

For the Bubnov-Galerkin formulation (standard finite element method) the weighting functions are set equal to the basis functions (Lagrange polynomials), i.e., $W_i = N_i$ for $i = 1, n_n$.

The formulation also makes use of the finite difference Crank-Nicolson, time-weighting scheme with parameter θ equal to 0.5 (semi-implicit scheme) chosen by experimentation. Let l and l+1 be the known and unknown time levels for the numerical scheme, and using a shorthand notation in which the set of n_n integrals is represented under the subscript I, equation 9 becomes:

$$\int_D N_I\left[\frac{\hat{h}^{\,l+1}}{\Delta t} + \theta\left(\frac{\partial \hat{q}^{\,l+1}}{\partial x} - i_e^{\,l+1}\right)\right] dx =$$

$$\int_D N_I\left[\frac{\hat{h}^{\,l}}{\Delta t} + (1-\theta)\left(\frac{\partial \hat{q}^{\,l}}{\partial x} - i_e^{\,l}\right)\right] dx \qquad (13)$$

Using equation 11, we can relate q to h. A modified Picard iteration scheme was chosen to solve the resulting system of non-linear equations in h. Defining m, m+1 as the last and current iteration, a linear set of equations results:

$$[A]\,\{h\}^{l+1,m+1} = \{b\} = \{b_o\}^l + \{b_m\}^{l+1,m} \qquad (14)$$

where [A] is a banded coefficient matrix that groups only linear terms in l+1, m+1 from equation 13, {b} is the vector that contains all the other terms, this is terms in l and l+1,m. The q terms are evaluated at the new time level, but lagged an iteration step, $q^{l+1,m}$, known after the initial and boundary condition 7 are applied. $\{b_o\}$ is the linear portion of {b}, and $\{b_m\}$ is the non-linear part. The matrix [A] is formed only once at the beginning of the numerical procedure, and a part of the vector {b} is calculated only once for each time step, $\{b_o\}$, and then modified by another part for each iteration step, $\{b_m\}$, until convergence for each time step was reached. As convergence criteria, we used (Huyakorn and Pinder, 1986):

$$\frac{\max_{j=1}^{n_n} \left| h_j^{\,l+1,m+1} - h_j^{\,l+1,m} \right|}{\max_{j=1}^{n_n} \left| h_j^{\,l+1,m+1} \right|} < \varepsilon \qquad (15)$$

where ε is arbitrarily set equal to 10^{-8} for the simulations.

The system 13 is solved for each iteration using a direct solver such as a Lower Upper Decomposition (LUD) algorithm for banded matrices.

Each of the terms of 12 was transformed to natural coordinates (ξ) and evaluated through a Gauss quadrature integration rule. The members of equation 14 result from the summation over the total number of elements (N_e) of elemental matrices and vectors:

$$[A] = \sum_{n_e=1}^{N_e} \left[A_e^{n_e}\right]$$

$$\{b_o\}^l = \sum_{n_e=1}^{N_e} \left\{b_{o_e}^{n_e}\right\}^l$$

$$\{b_m\}^{l+1,m} = \sum_{n_e=1}^{N_e} \left\{b_{m_e}^{n_e}\right\}^{l+1,m} \qquad (16)$$

where

$$\left[A_e^{n_e}\right] = \frac{\Delta x_{n_e}}{2\Delta t}\begin{bmatrix} \int_{-1}^{1} N_1 N_1 d\xi & \int_{-1}^{1} N_1 N_2 d\xi & \int_{-1}^{1} N_1 N_3 d\xi \\ \int_{-1}^{1} N_2 N_1 d\xi & \int_{-1}^{1} N_2 N_2 d\xi & \int_{-1}^{1} N_2 N_3 d\xi \\ \int_{-1}^{1} N_3 N_1 d\xi & \int_{-1}^{1} N_3 N_2 d\xi & \int_{-1}^{1} N_3 N_3 d\xi \end{bmatrix} \qquad (17)$$

$$\left\{b_{o_e}^{n_e}\right\}^l = \frac{\Delta x_{n_e}}{2} \times \qquad (18)$$

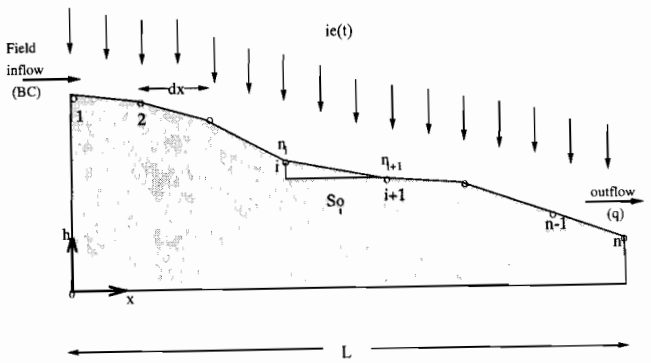

Figure 1–Field discretization for the finite element overland flow model.

$$\left\{\begin{array}{l}\displaystyle\int_{-1}^{1} N_1\left[\frac{\hat{h}^{\,l}}{\Delta t}+(1-\theta)\left(i_e^{\,l}-\frac{2}{\Delta x_{n_e}}\frac{\partial \hat{q}^{\,l}}{\partial \xi}\right)+\theta i_e^{\,l+1}\right]d\xi \\ \displaystyle\int_{-1}^{1} N_2\left[\frac{\hat{h}^{\,l}}{\Delta t}+(1-\theta)\left(i_e^{\,l}-\frac{2}{\Delta x_{n_e}}\frac{\partial \hat{q}^{\,l}}{\partial \xi}\right)+\theta i_e^{\,l+1}\right]d\xi \\ \displaystyle\int_{-1}^{1} N_3\left[\frac{\hat{h}^{\,l}}{\Delta t}+(1-\theta)\left(i_e^{\,l}-\frac{2}{\Delta x_{n_e}}\frac{\partial \hat{q}^{\,l}}{\partial \xi}\right)+\theta i_e^{\,l+1}\right]d\xi\end{array}\right\}$$

$$\left\{b_{m_e}^{n_e}\right\}^{l+1,m}=-\theta\left\{\begin{array}{l}\displaystyle\int_{-1}^{1} N_1\frac{\partial \hat{q}^{\,l+1,m}}{\partial \xi}d\xi \\ \displaystyle\int_{-1}^{1} N_2\frac{\partial \hat{q}^{\,l+1,m}}{\partial \xi}d\xi \\ \displaystyle\int_{-1}^{1} N_3\frac{\partial \hat{q}^{\,l+1,m}}{\partial \xi}d\xi\end{array}\right\} \qquad (19)$$

Table 1. Rainfall distribution used in simulations

Time (s)	Rainfall (m / s)
0	8.4667e–07
300	6.7733e–06
600	1.1007e–05
900	1.9473e–05
1200	1.9473e–05
1500	1.5240e–05
1800	5.0800e–06
2100	1.6933e–06
2400	2.5400e–06
2700	8.4667e–07
3000	0

Table 2. Range of parameters used in the simulations

Parameter	Symbol	Values	Comments
Surface roughness	n	0.04 0.4	Sparse vegetation Dense vegetation
Strip lengths	L	2,4,6,8,12,19	(m from field edge)
Strip Slope	S_o	1,2,4,6,8,10%	Slope
Soil Types	A, B	Sandy-loam, clay	See table 3

The values of i_e are calculated for each node and time step according to an infiltration equation (i.e., Green-Ampt) and a given hyetograph (described in the next section). The incoming hydrograph from the adjacent field is input as a time dependent boundary condition at the first node of the finite element grid. Any combination of unsteady storm and incoming hydrograph types can be used. The program allows for spatial variation of the parameters n and S_o over the nodes of the system (fig. 1). This feature of the program ensures a good representation of the field conditions for different rainfall events.

Infiltration Submodel: Modified Green-Ampt

The Green-Ampt infiltration model (Green and Ampt, 1911) was proposed as an application of Darcy's Law with the following simplifications: 1) homogeneous soil profile and uniform distribution of antecedent soil moisture; 2) the water moves in the soil in the form of an advancing wetting front and thus diffusion of soil moisture is neglected; 3) surface ponding. The equation is:

Table 3. Soil parameters used in the simulations

Layer*	Depth (cm)	Texture	p	e	db (g/cm^3)	ds (g/cm^3)	K_{sv} (cm / h)	K_{sh} (cm / h)	θ_s (cm^3 / cm^3)	θ_r (cm^3 / cm^3)	S_{av} (cm)	M (cm^3 / cm^3)	S_{av}.M (cm)
Soil A Data													
Ap†	0-23	SL	0.319	0.470	1.657	2.434	**6.02**	7.85	0.311	0.090	35.7	0.16	**5.71**
Bt1	23-41	C	0.298	0.380	1.610	2.221	4.78	4.74	0.436	0.147	1.8	—	—
Bt2	41-69	SC	0.442	0.795	1.348	2.420	4.93	2.02	0.376	0.129	31.4	—	—
Bt3	69-94	SCL	0.470	0.887	1.497	2.824	4.19	0.60	0.445	0.119	9.2	—	—
Soil B Data (Chu, 1978)													
Profile	—	C	—	—	—	—	**0.21**	—	—	—	—	—	**6.10**

* Nomenclature: p = Total porosity; e = Void ratio; db = Bulk density; ds = Particle density; S,C,L = Sand, clay, loam; K_{sv} = Vertical saturated conductivity; K_{sh} = Horizontal saturated conductivity; θ_s, θ_r = Saturated and residual water contents; S_{av} = Average suction at the wetting front; M = initial water content

† The Ap layer was the only one considered active for infiltration calculations.

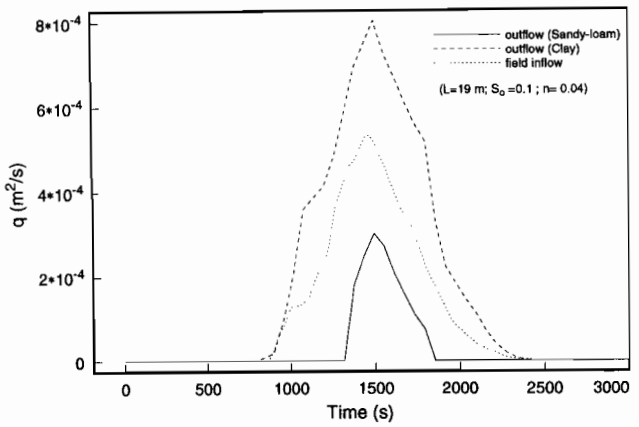

Figure 2a–Runoff event over a VFS with sparse grass for two types of soils.

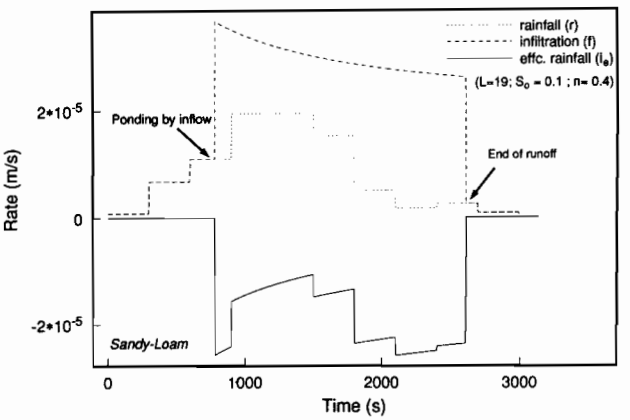

Figure 3–Water balance for the sandy-loam soil using the modified Green-Ampt model (storm on table 1).

$$f_p = K_s + \frac{K_s M S_{av}}{F_p} \qquad (20)$$

where f_p is the instantaneous infiltration rate, or capacity, for a ponded soil (m/s), K_s is the saturated hydraulic conductivity (m/s), $M = \theta_s - \theta_i$, is the initial soil-water deficit (m^3/m^3), S_{av} is the average suction across the wetting front (m), and F_p is the cumulative infiltration (m). This model does a good job describing infiltration during a rainfall event, with adequate estimation of the field parameters (Skaggs et al., 1969; Chu, 1978).

Mein and Larson (1971, 1973) applied the Green-Ampt model to natural rainfall conditions by integrating equation 20 with an initial condition that allows for some cumulative infiltration to occur before ponding. This yielded an implicit function of time:

$$K_s(t - t_p - t_s) = F - M S_{av} ln\left(1 + \frac{F}{M S_{av}}\right) \qquad (21)$$

where t is the actual time (s), t_p the time to ponding, and t_s is the shift of the time scale to the effect of having cumulative infiltration at the ponding time, or pseudotime.

The determination of the t_p and t_s parameters for an unsteady rainfall was described by Chu (1978). In this method, the unsteady storm is divided into constant rainfall periods. For each period a ponding indicator (C_u) is calculated to check if ponding at the surface at the end of the period is reached ($C_u > 0$) or not ($C_u < 0$) and its effect on infiltration:

$$C_u = P(t_n) - RO(t_{n-1}) - \frac{K_s M S_{av}}{r - K_s} \qquad (22)$$

where $P(t_n)$ is the total cumulative infiltration including the actual rainfall period and $RO(t_{n-1})$ is the total cumulative runoff (m), or cumulative rainfall excess, until the last rainfall period. At the beginning of the storm (no ponding) the value of C_u is checked. If no ponding at the end of the period occurs, the infiltration is set equal to rainfall ($i_e = 0$). If surface ponding occurs, it begins at t_p calculated as:

$$t_p = t_{n-1} + \left[\frac{K_s M S_{av}}{r - K_s} - P(t_{n-1}) + RO(t_{n-1})\right]\frac{1}{r} \qquad (23)$$

where $P(t_{n-1})$ and $RO(t_{n-1})$ are the total cumulative infiltration and runoff (m) until the last rainfall period and t_{n-1} is the time at the end of the last rainfall period. The pseudotime (t_s) can now be calculated from equation 21,

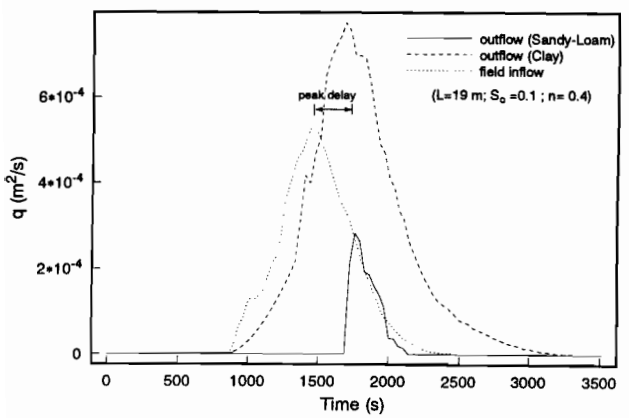

Figure 2b–Runoff event over a VFS with dense grass for two types of soils.

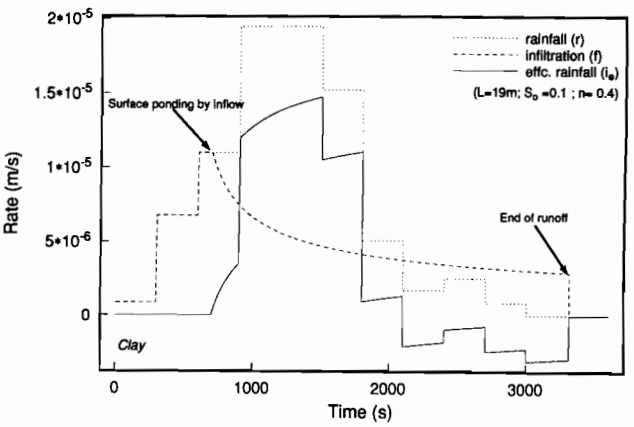

Figure 4–Water balance for the clay soil using the modified Green-Ampt (storm on table 1).

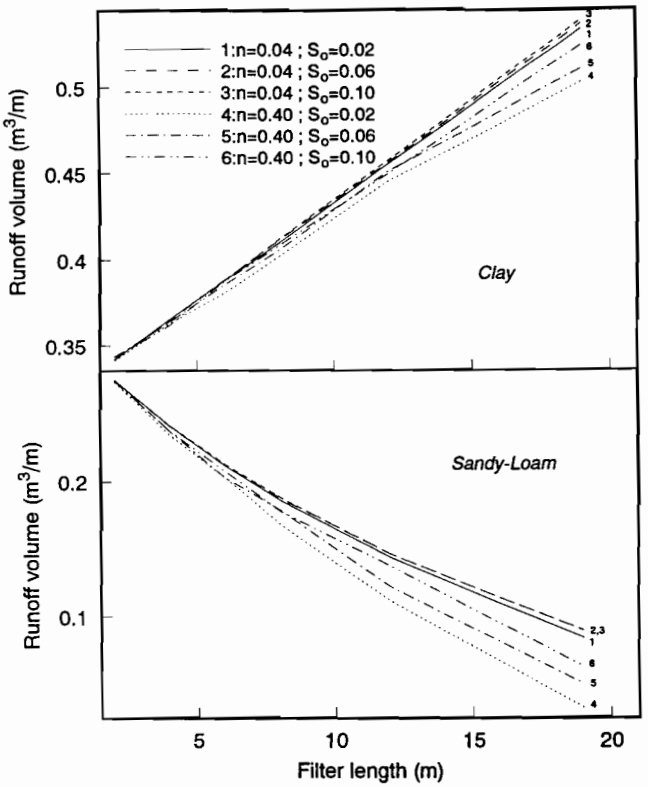

Figure 5–Effect of surface cover (roughness, *n*), field slope (S_o), and soil type on the total runoff volume.

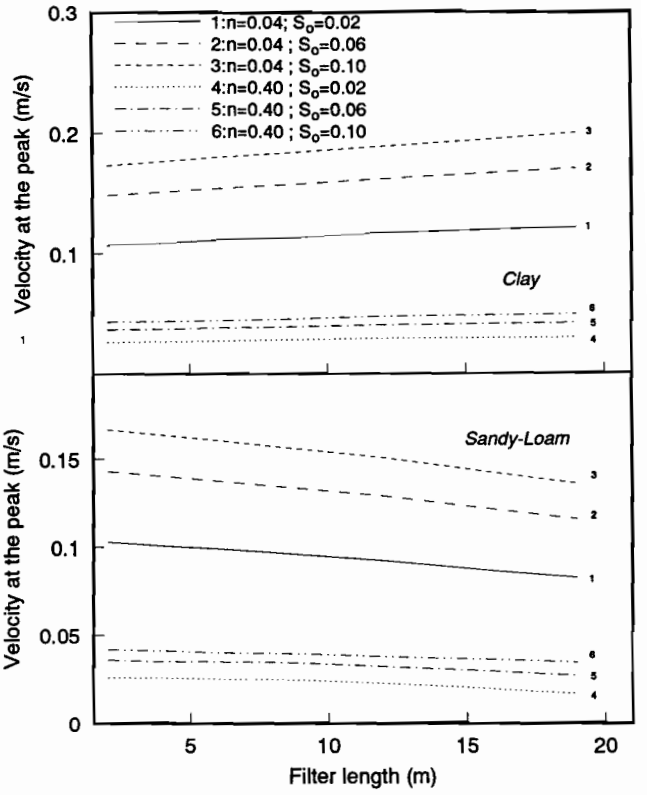

Figure 6–Effect of surface cover (roughness, *n*), field slope (S_o), and soil type on the peak velocity.

setting $F = F_p$ (from eq. 20). The calculation of the cumulative infiltration (F) requires an iterative method using equation 21. A Newton-Raphson non-linear solution procedure was used such as:

$$F_{m+1} = F_m - \frac{g(F_m)}{g'(F_m)} \qquad (24)$$

where g(F) is an implicit function in F derived from equation 21, i.e.:

$$g(F) = F - K_s(t - t_p - t_s) - MS_{av} ln\left(1 + \frac{F}{MS_{av}}\right) \qquad (25)$$

g′(F) its derivative, and the subscript m denotes the iteration level. The infiltration rate is calculated with equation 20 and then $i_e > 0$. If a new rainfall period starts with surface ponding, new parameters t_p and t_s are calculated and a check for the ponding status at the end of the period is done. If there is still ponding, infiltration and rainfall excess are calculated as above, otherwise, the infiltration is set to rainfall for the time after ponding ends. This procedure is repeated until the end of the storm.

The filter strip situation suggests several modifications to the above model. The most important one is that the major input for the overland flow is not rainfall as in a regular situation but the uphill field inflow. This is due to the relative difference in areas between field and filter strip, i.e., the field is typically from 3.5 to 7 times bigger than the buffer area (Parsons et al., 1990). Agricultural fields also display low infiltration rates (K_s) due to surface compaction. The basic assumption made here is that after the beginning of the runoff event, a moving film of water, coming mostly from the field, will be covering the surface (flood wave). This represents a sufficient volume to provide for the maximum potential infiltration. A further assumption of the model is that depressional storage (DS) effects are not considered important for the overall behavior of the filter. Filters should be settled and maintained over a fairly leveled area. The DS is less important than in the case of an agricultural field, since a uniform vegetation cover is maintained throughout the year and no cultural practices are applied. This assumption will be violated if channelization develops or the filter is otherwise eroded. The amount of water flooding the filter from the adjacent field will fill up any existing DS at the beginning of the runoff event, and will have little effect on the overland flow process afterwards

The infiltration submodel was formulated as follows:

- Rainfall starts. No uphill field inflow (delay). The boundary condition for the hydraulic routing submodel (BC) is set to 0. The VFS acts as an isolated soil. The Green-Ampt model is applied as described above and only the rainfall excess (ie), equally applied to every element of the system for each time step, is routed on the overland flow model.
- Field inflow starts. The BC at the first node of the system is changed for every time step following the inflow hydrograph. A check is made on the first and last node of the system (h values) to find flooding

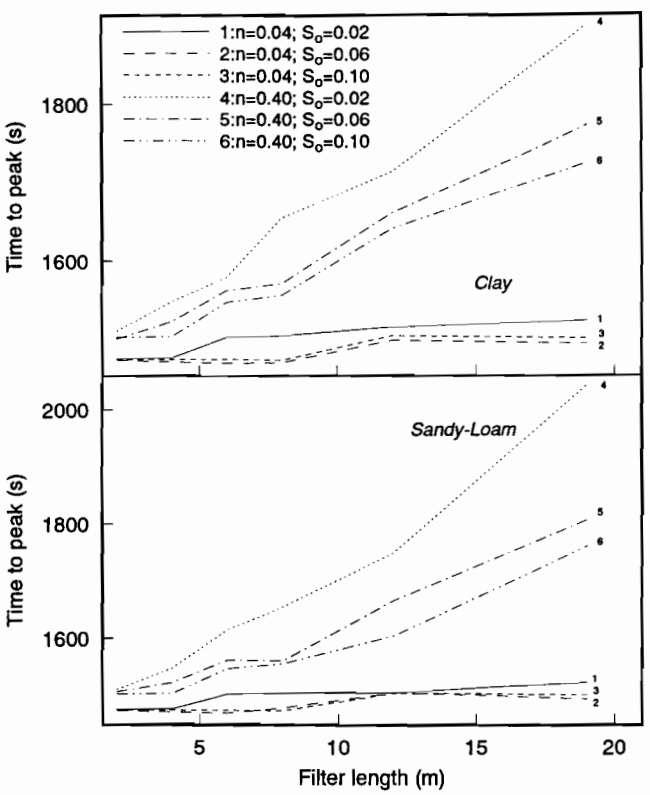

Figure 7–Effect of surface cover (roughness, *n*), field slope (S_o), and soil type on the time to peak.

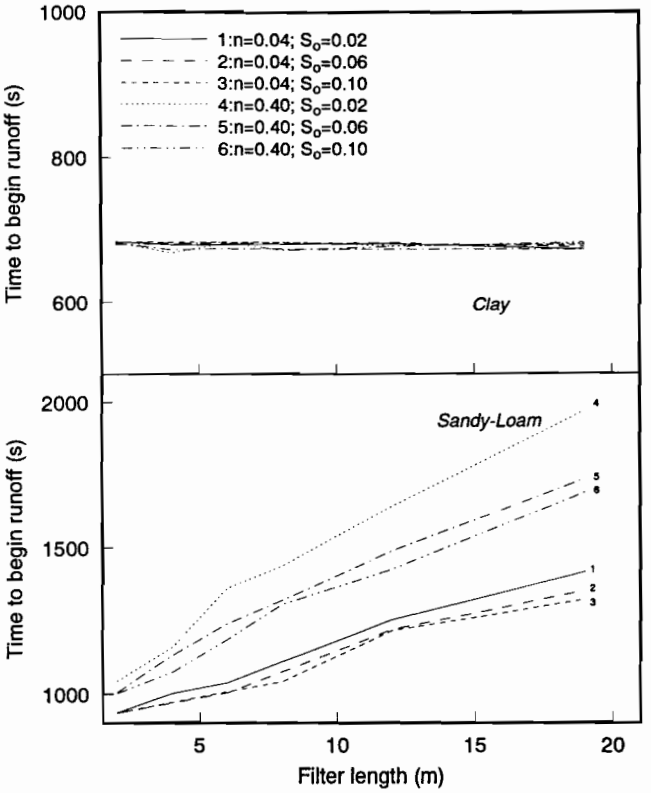

Figure 8–Effect of surface cover (roughness, *n*), field slope (S_o), and soil type on the time to start runoff.

of the surface by field inflow. At this time a signal is sent to the infiltration submodel to proceed as a ponded surface case, where the infiltration is allowed to reach its maximum, and the rainfall excess to be less than 0 in certain cases (rainfall is less than this assumed maximum infiltration). An example case is discussed in the next section to illustrate this point. This concept is important in order to explain the field experimental data where large reductions of the incoming flow rate are obtained at the end of the filters (Parsons et al., 1990).

- Field inflow stops, the BC is set back to 0 and a signal is sent to the infiltration subroutine to proceed as the normal case until the end of the storm.

The above procedures show how different soil types are handled by the model through the Green-Ampt parameters (K_s, M, S_{av}).

Model Application

A set of 144 simulations was conducted for a range of parameters to compare filter strip performance. A summary of the inputs used is given in tables 1 through 3. Two soil types, A and B were selected. Soil A is of sandy-loam texture at the surface. This surface layer controls infiltration. Field and lab tests were conducted on this soil. Soil B, in contrast, is a deep homogeneous clay soil (Chu, 1978). The soil parameters for the simulations are included in table 3.

The effect of the different hydraulic properties of each of these soils is illustrated in figures 2a and 2b. These graphs were obtained using the assumptions discussed for the infiltration submodel and for the storm event in table 1. The sandy-loam soil shows a marked reduction in total runoff (area under the q curve), as compared to field inflow, due to infiltration. Conversely, the clay soil shows an increase in runoff due to the addition of the rainfall atop to the runoff flow and the small infiltration capacity. These figures also illustrate the effect of vegetation type (Manning's n) on the outflow. For the dense grass (n = 0.4), there is a distinctive delay in the time to reach the q-peak. Figures 3 and 4 show the water balance, as given by the infiltration submodel, for both soils and the case depicted on figure 2b. When the surface starts to be inundated by the flood wave, the maximum potential infiltration is achieved. The difference between the two soils can be seen in terms of the effective infiltration values (i_e). Soil A has high rates of infiltration (i_e mostly negative). Soil B is less permeable (i_e mostly positive) resulting in different filter behavior.

Soil type has the biggest effect on runoff volume (fig. 5), q_{vol}(m^3/m filter width), and depth-averaged velocity at the peak (fig. 6), v_{peak} (m/s). The trend in these results (regardless of n and S_o combinations) is inverted, i.e., for soil A the runoff volume decreases with length whereas it increases with soil B. The sandy-loam acts as a predominantly infiltrating media for this event. Thus, as the area (length) increases, the mass of water entering the soil profile increases, reducing the runoff volume. In the clay (soil B) as the area increases, the catchment of direct rainfall also increases and, since infiltration is minimal, the runoff volume increases. In both cases, as the length of the filter approaches zero, the volume equals that of the inflow from the adjacent field (0.32 m^3/m). The effect of grass

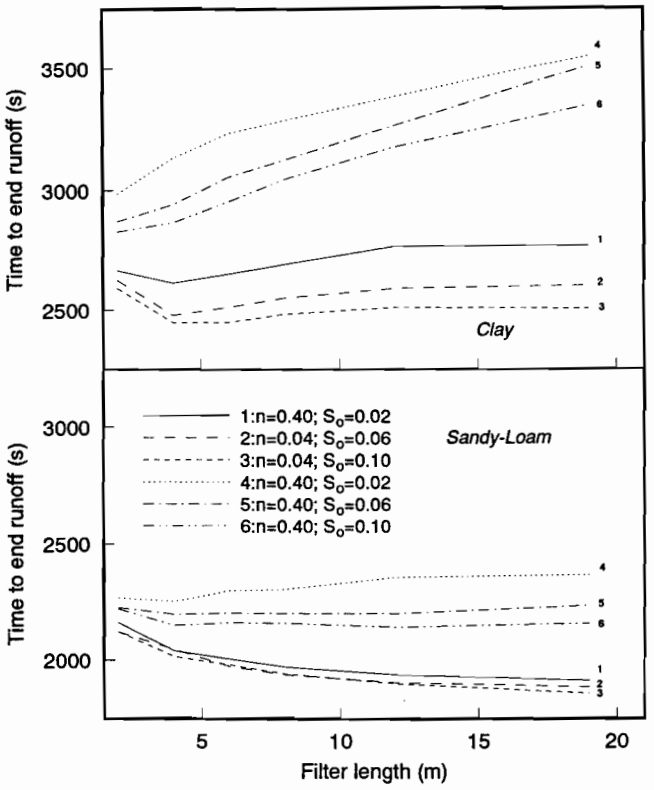

Figure 9–Effect of surface cover (roughness, *n*), field slope (S_o), and soil type on the time to end runoff.

density (n) and slope (S_0) was very similar for both soil types. The retardation of the flow produced by a dense grass stand and small slope slightly increased infiltration. This combination yielded the lower runoff volumes in each soil. For the same grass density, decreasing the slope results in smaller volumes. Velocity at the peak flow is also reduced by the above combination (fig. 6).

The time to peak(s) is not significantly affected by soil type but rather by the roughness-slope combination (fig. 7). The greater the resistance to flow and the smaller the slope, the longer it will take for the hydrograph to reach its peak with similar times for both soils. Therefore, a delay in reaching the peak could be extended by manipulating the properties of the filter (long filter, small slope, dense vegetation) to a point where the direct rainfall has stopped, thus reducing the flow wave.

The time to the beginning of the runoff event(s) is affected by soil type (fig. 8). For soil A, denser grass and smaller slope delays the beginning of the event. Again, more water is infiltrated before ponding at the surface is reached. For the clay (soil B), there is no significant change in this value for any of the parameter combinations.

The tail of the hydrograph (time to end) is different for each combination of parameters (fig. 9). For soil A and sparse vegetation, there is a decrease in the time as L and S_0 increase. For the dense vegetation the effect of length is insignificant. For soil B, and sparse grass, L does not influence the time to end after 4 m, but it takes longer to reach the end of the hydrograph (around 2600 s compared to 2200 s for soil A).

Conclusions

A numerical model to study and simulate flow in Vegetative Filter Strips is presented. The model is composed of two submodels. A kinematic wave approximation for overland flow is solved numerically with quadratic finite elements. A second submodel describes infiltration for unsteady rainfall, based on the Green-Ampt equation, provides mass balance for the system. The infiltration equation is solved iteratively for each time step and the resulting effective rainfall value is fed to the numerical overland flow model at each time step.

Several field parameters can be specified in the model. These include slope, surface cover, length of filter and soil type. The model also handles natural rainfall events and inflow from an adjacent field, thus providing great flexibility for analysis of events.

Different combinations of the input parameters were selected for analysis. The results show the importance of soil type in runoff formation on the filters. Filter performance, i.e., reduction of the runoff volume and velocity, is higher for denser grass cover, smaller slopes, and soils with higher infiltration capacity. The runoff volume and velocity at the peak of the hydrograph could increase or decrease with length of the filter depending on soil type (high and low infiltration capacities, respectively). The velocity of the flow is mainly controlled by slope and density of the vegetation, where denser and smaller slopes give the smallest values. The time to beginning of runoff is soil dependent, i.e., length of the filter does not affect this parameter for soils with low infiltration capacity.

Management practices for the buffer areas could be suggested in the light of these results. If the clay content of the soils is high, any practice to improve infiltration is advisable. Special care should be given at the time of implantation of the buffers (leveling of the surface to a small slope in the buffers, dense grass, subsoiling, etc.) and later avoiding any activities that could compact the areas, such as traffic.

Acknowledgements. This study is supported in part by USDA-SCS, US-EPA, NC-WRRI, and Southern Region Project S249. The first author wishes to express appreciation for the economic support he is receiving as a Fellow of the *Instituto Nacional de Investigaciones Agrarias of Spain* (INIA). Thanks also to Mr. Charles A. Williams and Ms. Brenda Mason for their help.

References

Bedient, B. P. and W. C. Huber. 1988. *Hydrology and Floodplain Analysis*. New York: Addison Wesley.

Blandford, G. E. and M. Meadows. 1990. Finite element simulation of non-linear kinematic surface runoff. *J. Hydrol* 119:335-356.

Brakensiek, D. L. 1967. Kinematic flood routing. *Transactions of the ASAE* 10(3):340-343.

Bras, L. R. 1990. *Hydrology: An Introduction to Hydrological Science*. New York: Addison Wesley.

Chu, S. T. 1978. Infiltration during unsteady rain. *Water Resour. Res.* 14(3):461-466.

Cundy, T. W. and S. W. Tento. 1985. Solution to the kinematic wave approach to overland flow routing with rainfall excess given by Phillip's equation. *Water Resour. Res.* 21(8):1132-1140.

Eagleson, P. S. 1970. *Dynamic Hydrology*. New York: McGraw-Hill Book Co.

Eggert, K. G. 1987. Upstream calculation of characteristics for kinematic wave routing. *J. of Hydr. Eng. ASCE.* 113(6):743-752.

Engman, E. T. 1986. Roughness coefficients for routing surface runoff. *J. Irrigation and Drainage Eng. ASCE* 112(1):39-53.

Flanagan, D. C., G. R. Foster, W. H. Neibling and J. P. Burt. 1989. Simplified equations for filter strip design. *Transactions of the ASAE* 32(6):2001-2007.

Foster, G. R. 1982. Modeling the erosion process: Upland erosion. In *Hydrologic Modeling of Small Watersheds*, ed. C. T. Haan, H. P. Johnson and D. L. Brakensiek, 304-312. St. Joseph, MI: ASAE.

Foster, G. R. and L. D. Meyer. 1972. Transport of soil particles by shallow flow. *Transactions of the ASAE* 15(1):99-102.

Green, W. H. and G. Ampt. 1911. Studies in soil physics, Part I. The flow of air and water through soils. *J. Agricultural Sci.* 4:1-24.

Henderson, F. M. and R. A. Wooding. 1964. Overland flow and ground water flow from a steady rainfall of finite duration. *J. Geophys. Res.* 69(8):1531-1540.

Henderson, F. M. 1966. *Open Channel Flow*. New York: McMillan.

Horton, R. E. 1945. Erosional development of streams and their drainage basins, hydrophysical approach to quantify morphology. *Bull. Geol. Soc. of Amer.* 56:275-370.

Huyakorn, P. S. and G. F. Pinder. 1986. *Computational Methods in Subsurface Flow*. San Diego: Academic Press.

Izzard, C. F. 1946. Hydraulics of runoff from developed surfaces. In *Proc. 26th Annual Meeting of the Highway Research Board* 26:126-146.

Judah, O. M. 1972. Simulation of runoff hydrographs from natural watersheds by finite element method. Ph.D. diss., Virginia Polytechnic Institute and State University, Blacksburg.

Lane, L. J., G. R. Foster and A. D. Nicks. 1987. Use of fundamental erosion mechanics in erosion prediction. ASAE Paper No. 87-2540. St. Joseph, MI: ASAE.

Lane, L. J. and D. A. Woolhiser. 1977. Simplifications of watershed geometry affecting simulation of surface runoff. *J. Hydrol.* 35:173-190.

Ligget, J. A. and D. A. Woolhiser. 1967. The use of the shallow water equations in runoff computation. In *Proc. 3rd Annual Amer. Water Resources Conf.*, 117-126. San Francisco, CA: AWRA.

Lighthill, M. J. and C. B. Whitham. 1955. On kinematic waves: Flood movement in long rivers. In *Proc. R. Soc. London Ser. A* 22:281-316.

Mein, R. G. and C. L. Larson. 1971. Modeling the infiltration component of the rainfall-runoff process. Bulletin 43. Minneapolis, MN: Water Resources Research Center, Univ. of Minnesota.

Mein, R. G. and C. L. Larson. 1973. Modeling infiltration during a steady rain. *Water Resourc. Res.* 9(2):384-394.

Muñoz-Carpena, R., C. T. Miller and J. E. Parsons. 1993. A quadratic Petrov-Galerkin solution for kinematic wave overland flow. *Water Resources Res.* (In press).

Panda, J. C., S. A. Nielsen and I. D. Moore. 1988. A hydrological model for small agricultural catchments in the semiarid tropics. In *Modeling Agricultural Forest and Rangeland Hydrology*, ed. ASAE. St. Joseph, MI: ASAE.

Parsons, J. E., R. D. Daniels, J. W. Gilliam and T. A. Dillaha. 1990. Water quality impacts of vegetative filter strips riparian areas. ASAE Paper No. 90-2501. St. Joseph, MI: ASAE.

Ponce, V. M. 1991. The kinematic wave controversy. *J. Hydraulic Eng. ASCE* 117(4):511-525.

Rawls, W. J. and D. L. Brakensiek. 1988. An infiltration model for evaluation of agricultural and range management models. In *Modeling Agricultural Forest and Rangeland Hydrology*, ed. ASAE. St. Joseph, MI: ASAE.

Richards, L. A. 1931. Capillary conduction of liquids in porous mediums. *Physics* 1:318-333.

Ross, R. B. 1977. Finite element simulation of overland flow and channel flow. *Transactions of the ASAE* 20(4)705-712.

Ross, R. B., D. N. Contractor and V. O. Shanholtz. 1979a. A finite element model of overland and channel flow for assessing the hydrologic impact of land-use change. *J. Hydrol.* 41:11-30.

Ross, R. B., V. O. Shanholtz and D. N. Contractor. 1979b. A spatially responsive hydrologic model to predict erosion and sediment transport. *Water Resources Bulletin, AWRA* 16(3):538-545.

Schmid, B. H. 1989. On overland flow modeling. Can rainfall excess be treated as independent of flow depth? *J. Hydrol.* 107:1-8.

Skaggs, R. W., L. E. Huggins, E. J. Monke and G. R. Foster. 1969. Experimental evaluation of infiltration equations. *Transactions of the ASAE* 12(6):822-828.

Skaggs, R. W. and R. Khaheel. 1982. Infiltration. In *Hydrologic Modeling of Small Watersheds*, ed. C. T. Haan, H. P. Johnson and D. L. Brakensiek, 139-149. St. Joseph, MI: ASAE.

Springer, E. P. and T. W. Cundy. 1988. The effects of spatially varying soil properties on soil erosion. In *Modeling Agricultural Forest and Rangeland Hydrology*. St. Joseph, MI: ASAE.

Stone, J. J., L. J. Lane and E. D. Shirley. 1992. Infiltration and runoff simulation on a plane. *Transactions of the ASAE* 35(1):161-170.

Swift, L. W. 1986. Filter strip widths for forest roads in the southern Appalachian. *Southern J. Appl. For.* 10:27-34.

Vieux, B. E. 1988. Finite element analysis of hydrologic response areas using geographic information systems. Ph.D. diss., Michigan State University, East Lansing.

Vieux, B. E., V. F. Bralts, L. J. Segerlind and R. B. Wallace. 1991. Finite element watershed modeling: One-dimensional elements. *J. Water Resour., Planning and Mgmt. Div. ASCE* 116(6):803-819.

Vieux, B. E. and L. J. Segerlind. 1989. Finite element solution accuracy of an infiltrating channel. In *Proc. 7th Int. Conf. on Finite Element Methods in Flow Problems*. Huntsville, AL: University of Alabama.

Woods, R. A. and R. P. Ibbitt. 1988. Analytical solution for kinematic flow over an infiltrating plane. In *Modeling Agricultural Forest and Rangeland Hydrology*. St. Joseph, MI: ASAE.

Woolhiser, D. A. 1975. Simulation of unsteady overland flow. In *Unsteady Flow in Open Channels*, Vol. II, ed. K. Mahmood and V. Yevjevich, 485-508, Fort Collins, CO: Water Resources Publications.

Woolhiser, D. A., J. A. Liggett. 1967. Unsteady, one-dimensional flow over a plane, the rising hydrograph. *Water Resources Res.* 3(3):753-771.

Woolhiser, D.A., R.E. Smith and D.C. Goodrich. 1990. KINEROS, A Kinematic Runoff and Erosion Model: Documentation and User Manual. USDA-ARS. ARS-Publication No. 77.